


RESEARCH

Open Access



Improving household water treatment: using zeolite to remove lead, fluoride and arsenic following optimized turbidity reduction in slow sand filtration

Charles Onyutha^{1*} , Emmanuel Okello¹, Rebecca Atukwase¹, Pamela Nduhukiire¹, Michael Ecodu¹ and Japheth Nkiriyehe Kwiringira²

Abstract

Despite the United Nations 2030 agenda, large number of both urban and rural dwellers in low-income countries continue to lack access to improved water. Thus, increased effort is required towards enhancing low-cost drinking water treatment technologies especially for developing countries. Slow sand filter (SSF) is one of the most commonly used low-cost and efficient technologies for treating household drinking water. However, effectiveness of SSF is substantially affected by very high turbidity and relatively large amounts of dissolved heavy metals. To enhance removal of both turbidity and heavy metals, this study optimized sand bed depth (SBD) of SSF and investigated the potential of natural zeolite from Uganda for removal of lead, arsenite (As(III)) and fluoride ions from water. To remove lead ions, the zeolite was used in its natural form. However, to remove As(III) and fluoride, the natural zeolite was modified using hexadecyltrimethylammonium bromide solution. Removal of high turbidity was found to require a large optimal SBD. Furthermore, efficiency of treating synthetic turbid water increased with increasing initial turbidity. Variation of final turbidity with SBD was found to be best described by an exponential function. Optimal SBDs on top of an underdrain gravel layer of 0.2 m were 453, 522, 561, and 580 mm for turbidity of 60, 80, 100, and 120 NTU, respectively. Optimized SBD used achieve at least 95% efficiency in removing suspended particles from water with turbidity 120 NTU was found to save up to 35% of the total cost for acquiring sand volume required by a conventional SSF. For a particular zeolite mass, removal efficiencies of lead, As(III) and fluoride generally increased with increasing contact time. Removal efficiencies of lead, As(III), and fluorides were also shown to increase with increasing zeolite mass. Lead removal efficiencies using natural zeolite were 75 and 98% under 20 and 40 min, respectively. Removal of As(III) using modified zeolite mass was 91% within contact time of 10 min. Adsorption of fluoride on modified zeolite was 80% within 5 min. Adsorption of lead, As(III), and fluorides indicated promising potential of natural zeolites from Uganda for treating polluted water.

Keywords Water treatment, Slow sand filter, Turbidity removal, Heavy metal removal, Ugandan natural zeolite, Modified zeolite, Fluoride ions removal, Household water treatment

*Correspondence:

Charles Onyutha

conyutha@kyu.ac.ug

Full list of author information is available at the end of the article



© The Author(s) 2024. **Open Access** This article is licensed under a Creative Commons Attribution 4.0 International License, which permits use, sharing, adaptation, distribution and reproduction in any medium or format, as long as you give appropriate credit to the original author(s) and the source, provide a link to the Creative Commons licence, and indicate if changes were made. The images or other third party material in this article are included in the article's Creative Commons licence, unless indicated otherwise in a credit line to the material. If material is not included in the article's Creative Commons licence and your intended use is not permitted by statutory regulation or exceeds the permitted use, you will need to obtain permission directly from the copyright holder. To view a copy of this licence, visit <http://creativecommons.org/licenses/by/4.0/>.

1 Introduction

The need for each local community to have access to an improved water quality ranked high on the United Nations 2030 agenda [1]. Thus, Target 6.1 of the United Nations Sustainable Development Goal is to “achieve universal and equitable access to safe and affordable drinking water for all by 2030” [1]. However, the press release of the joint monitoring programme of the World Health Organization (WHO) and United Nations Children’s Fund (UNICEF) on 1st July 2021 was titled “*Billions of people will lack access to safe water, sanitation and hygiene in 2030 unless progress quadruples – warn WHO, UNICEF*”. Furthermore, despite the United Nations 2030 agenda, the population in low-income countries that had access to improved water (or potable water readily available on household premises) by 2020 was only 28.8% (see details via <https://ourworldindata.org/clean-water-sanitation> [accessed: May 26 2023]). Thus, there is a need for increased effort towards low-cost drinking water treatment to increase access to safe potable water in low-income countries. The need to optimize efficiency of household water treatment is linked to the importance of increasing access to affordable drinking water for vulnerable communities [2]. Some of the major drinking water quality issues in developing countries include turbidity and presence of heavy metals.

Slow sand filter (SSF) is one of the most commonly used and efficient technologies for reducing turbidity and removal of pathogens in drinking water. *Schmutzdecke* (a thick biofilm layer at the surface of the SSF) has commendable capacity to remove pathogens such as bacteria and protozoa but it can considerably contribute to total head loss through overgrowth of the biofilm. Performance of SSF depends on a number of factors such as depth of the filtration media, the influent loading rate (or $L d^{-1} m^{-2}$), and level of contamination of the raw water to be treated. One source of high turbidity is clay which tends to get into the water due to erosion especially during rainy season. Before using SSF for treating highly turbid raw water ($>> 25$ NTU), pretreatment is required. Furthermore, conventional SSF has reduced capacity to remove heavy metals.

The presence of fluorides and heavy metals in the environment comprises another major concern for drinking water treatment. Sources of heavy metals in the environments include mining, and other industrial operations. Some heavy metals commonly found in polluted water include zinc, lead, arsenic, manganese, cadmium, and chromium. SSF is suggestively a useful method for the removal of dissolved heavy metals [3]. However, the raw water which has dissolved heavy metals should be avoided if the SSF is without roughing filter pretreatment [4]. Heavy metals when ingested can cause several

diseases [5]. Furthermore, heavy metals can be carcinogenic, mutagenic, and incurable with various negative effects on kidney and other organs of the body [6]. The presence of arsenic in drinking water is a world-wide concern [7]. Arsenic in drinking water can cause bladder, lung, and non-melanoma skin cancer [8]. In some parts of the world, such as in Tororo district at the Sukulu highlands in Uganda [9] fluorides can be used as food additive. While fluorides aid in preventing dental decay, excessive fluoride consumption can cause parathyroid gland injury, and fluorosis of teeth and skeleton.

There are various adsorbents such as zeolite and activated carbon that can be used for adsorption of dissolved heavy metals in water. Activated carbon is the oldest and most well-known adsorbent in water treatment; however, it is expensive, and improvement of its adsorption capacity requires complicated auxiliary. The cost of applying zeolite for water treatment is relatively low [10]. The cost of zeolite as an adsorbent is < 1 USD mol^{-1} and this is far less than that for activated carbon [11]. Detailed comparison of zeolite with other adsorbents under various circumstances such as cost of preparation and application can be found in a recent study [11]. Zeolites can occur naturally as crystalline aluminosilicates [10]. In other words, zeolites are aluminosilicates with negatively charged micro pore frames that can accommodate molecules for chemical reaction catalysis and environmental clean-up [12]. The high particle porosity, low tendency in clogging up, and commendable effective surface area altogether make zeolite to have great capacity as an adsorption agent. Thus, zeolite can adsorb large amounts of pollutants before requiring backwashing, and it does not lead to large pressure drop while used for water treatment.

Developments regarding the need to improve SSF especially with respect to filter design and physicochemical processes incurred during filtration are lacking [2]. In this line, the first knowledge gap that this study focused on concerned sand depth optimization (SDO) for efficient turbidity removal. The second gap was on the need to enhance the capacity of SSF in removal of heavy metals and halides.

In regard to the first aim of this study, turbidity was considered because it is a major concern in determining the quality of drinking water in developing countries. Furthermore, turbidity also influences the decrease of discharge from the SSF with time. This is because, turbidity removal varies with the sand depth in SSF. Optimal sand depth (s_{opt}) is important for determining the size of portable SSFs given the easy-to-obtain materials including buckets, sand, polyvinyl chloride pipes, and concrete. Furthermore, s_{opt} can reduce the need for pretreatment especially for a known range of turbidity values.

The second aim of this study focused on investigating the potential of zeolite for removal of fluorides and heavy metals especially As(III) and lead ions from drinking water. There are various techniques available for removal of heavy metals from water including ion-exchange, adsorption, extraction, and membrane processes [10]. Regarding fluorides, various defluoridation techniques exist such as reverse osmosis, nano filtration, dialysis, and electro dialysis [6]. However, majority of these techniques are expensive to utilize on a community and household basis in low resource settings [13]. Adsorption is a relatively cheap technique for removal of fluorides [6] and heavy metals from drinking water and this makes it a viable proposition. Adsorption is also preferred to other methods because of its simplicity.

The idea behind optimized turbidity reduction followed by the use of zeolite to remove various adsorbates in drinking water is to enhance efficiency of low-cost method of disinfection especially chlorination that is normally used in developing countries. The point is that suspended particles responsible for causing turbidity tend to harbor large number of pathogenic microbes. If water at the point of chlorination still has large number of pathogenic microbes, the capacity of the residual chlorine for disinfection is greatly reduced. Therefore, turbidity should be substantially reduced so as to greatly lower the number of pathogens in the water before the point of chlorine dosage. For this study, we considered raw water source in the form of surface rainfall-runoff impounded in an earth dam at Kamuli, in Uganda. This dam was considered because it provides raw water that is treated using SSF and supplied to several villages. Furthermore, daily values of observed turbidity of polluted water from the selected dam before and after treatment using SSF during both dry and wet seasons were available at the parastatals in Uganda. The SDO for a laboratory-scale SSF was based on synthetic turbid water with suspended particles comparable with the range of observed turbidity levels. The natural zeolite used for adsorption experiments in this study was obtained from Mbale district in the eastern Uganda. For removal of lead ions, zeolite performs well in its natural form. However, unmodified zeolite is known to exhibit minimal capacity to remove fluoride [14] and arsenic [15]. Thus, zeolite was modified for improved removal of fluoride and As(III) from water.

2 Materials and methods

2.1 Determining water turbidity

2.1.1 Actual water turbidity

Actual turbidity was obtained from the rainfall-runoff impounded into an earth dam from which raw water for Kamuli water treatment plant in the eastern Uganda

is drawn. Raw water was sampled from the dam in the morning (8:00 am), afternoon (12:30 pm), and evening (6:00 pm) of each day in February, March, April, and May 2022. Also, the filtered water from the SSF was sampled on a daily basis. Turbidity in each water sample was tested using the procedure from ISO 7027-1:2016 standard accessible via <https://www.iso.org/standard/62801.html> (accessed: 24th November, 2023). Turbidity values of water before and after SSF were compared. In the study area, February falls within a dry season. However, March, April and May comprise the main rainy season. Capturing a wide range of turbidity levels over both dry and wet season was deemed important for generating realistic synthetic turbid water for laboratory-scale experiment.

2.1.2 Synthetic turbid water

Different clay soil samples with masses in the range 0–1.6 mg were considered. Each soil sample was dissolved in 1 L of distilled water to create synthetic turbid water. Clay soil suspension was subjected to quick mechanical agitation (300 rpm) for 5 min in a jar test device, followed by 30 min of gentle mixing (40 rpm). This was to achieve a homogeneous dispersion of clay particles. In the next step, the solution was left to settle for 10 min. Turbidity of the supernatant liquors was measured and quantified in NTU in accordance with ISO 7027:2016 standard (see details via <https://www.iso.org/standard/62801.html> [accessed: 24th November 2023]). For every selected mass of clay soil, the experiment was conducted twice and the average of the two turbidity values was reported. Scatter plot of clay soil masses versus resultant turbidity values was made. A regression line characterizing the variation of observed turbidity (NTU) with clay soil mass (mg L^{-1}) was fitted to the plot to generate an equation to determine the clay masses for selected turbidity values for the SDO experiment.

2.1.3 Experimental set up for optimizing sand depth

Four SSF metallic prototypes each with $300 \times 300 \times 1700$ mm dimension and locally fabricated in Bukasa Kirinya Kampala, Uganda, were used in this study. The photograph and the longitudinal section of the metallic prototypes are shown Fig. 1a and b, respectively. These prototypes were fitted with adjustable valve systems for draining the filtered water. The volume of thoroughly washed sand with particle effective size in the range 0.18–0.30 mm and uniformity coefficient of 1.8 was measured using a clean batch box of $300 \times 300 \times 300$ mm dimension. The SSF prototypes were thoroughly washed and ensured to be clean before placing the sand. The height of underdrain including gravel layer was 200 mm. The clean sand was packed onto the gravel and

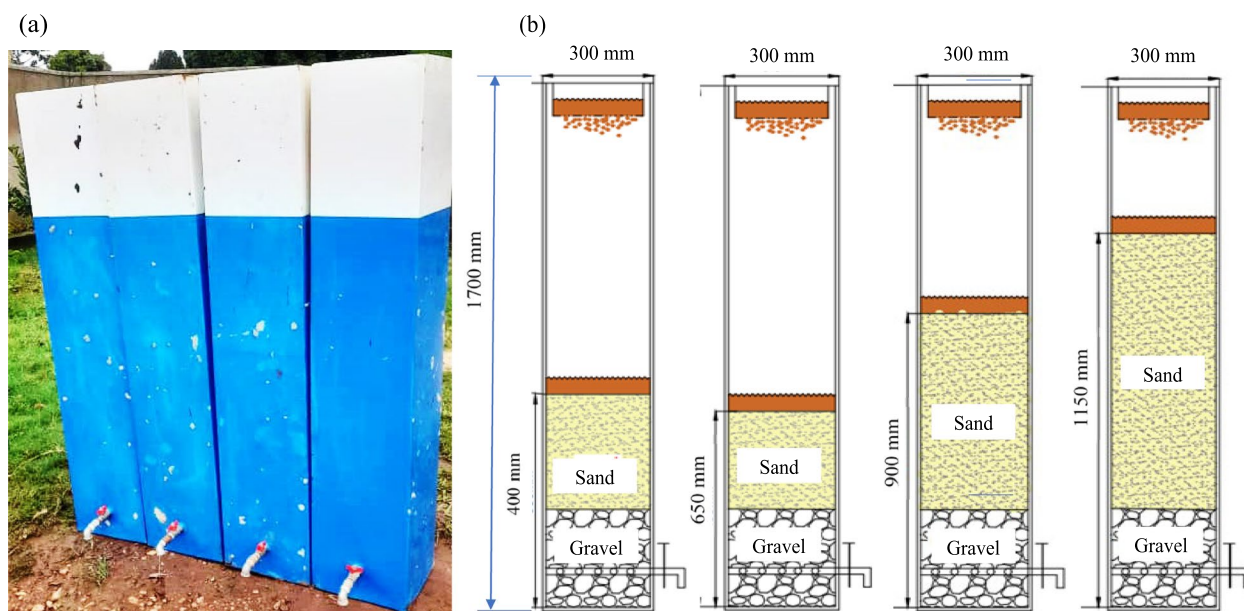


Fig. 1 Experimental setup in terms of (a) photograph of the physical prototypes, and (b) and illustration of the experimental set up

underdrain at various depths including 200, 450, 700, and 950 mm (Fig. 1). Filtration rate may be regulated either at the inlet (inlet control) or at the outlet (outlet control). Pilot testing was done using hydraulic loading rate of $0.2 \text{ m}^3 \text{ h}^{-1} \text{ m}^{-2}$. For actual experiments, the outlet control was adopted in line with the need to test for possibility of providing daily flow regulation.

Synthetic water with any of known turbidity levels (5–120 NTU) was fed into each SSF prototype. The time taken to obtain one L of filtered water was noted. The turbidity level in the filtered water was measured in NTU. The difference between the initial turbidity (T_1) and turbidity after filtration as a percentage of T_1 was taken as the removal efficiency. For each known turbidity, the experiment was repeated at least three times. The average turbidity removal efficiencies was considered.

In SDO, final turbidity values above 5 NTU were considered. Following the information via <https://www.who.int/publications/i/item/9789240045064> [accessed: 19th November 2023]), the 5 NTU is WHO recommended limit (denoted hereafter as W-Rlim) of turbidity in drinking water. Scatter plots of turbidity values versus sand depths were made. To each scatter plot, various models in the forms of logarithmic, linear, power and exponential equations were fitted. Model performance was evaluated in terms of the mean squared error (MSE). The best model was the one with the smallest MSE value and it was used to determine the s_{opt} or the sand bed depth which led to reduction of the T_1 values from the range 5–120 NTU to ≤ 5 NTU.

2.2 The use of zeolite for water treatment

2.2.1 Presence of heavy metals in water

Raw water samples were drawn from the dam at Kamuli in the eastern Uganda. The presence of arsenic, lead, manganese, cadmium, chromium, cobalt, copper, and iron were tested. Laboratory testing was done using an Atomic Absorption Spectroscopy (AAS) machine 200 series following the 24th edition of the American Public Health Association (APHA) Standard Methods for the Examination of Water and Wastewater.

2.2.2 Characterization of zeolite

Natural zeolite samples were extracted from Mbale district, particularly in Wanale sub-county of the Mount Elgon region in eastern Uganda. Pieces of natural zeolite of varying sizes were crushed using a hammer mill to a mesh size of less than 500 μm . This was followed by dry milling using a ball mill (PM100, Retsch Co.), rotating at 650 rpm for 3 min with ball to powder ratio of 2:3 up to a mesh size 75 μm . No chemicals were added to this zeolite.

To determine the metal oxides (Silica and Alumina), 1 g of zeolite was weighed and placed in a 100 mL beaker. It was mixed with 10 mL of strong hydrochloric acid and dried in a fume hood using an electric hotplate. Next, 30 mL of distilled water and an additional 6 mL of hydrochloric acid were added. The liquid was heated to boiling point. The hot solution was filtered through ash-less filter paper, and the precipitate was rinsed with 30 mL of hot distilled water. The filtrate was preserved to estimate the iron and aluminum. The precipitate and

filter paper were transferred to a clean and weighed crucible. The crucible and its contents were burned to 800 °C for 50 min and the crucible was left to cool in the dryer and weighed. Proportion of the silicon oxide was calculated as the ratio of the weight of silicon oxide to the sample weight in percentage.

To determine the mixed oxides (Al_2O_3 and Fe_2O_3), the filtrate left after precipitation of silica was diluted to around 200 mL in a beaker. It was heated to boiling point after adding 2 g of ammonium chloride and a few drops of methyl red indicator. The color was gradually turned yellow by the use of ammonia solution. After 10 min, the solution was filtered through ash-free filter paper, and 2% ammonium nitrate solution was used to wash the precipitate and filter paper. A clean, weighed crucible was used to hold the precipitate and filter paper. The crucible and its contents at 800 °C were burnt for 50 min. After cooling in the dryer, the crucible was weighed to calculate the mixed oxides.

To compute the percentage of ferric oxide, 5 mL of strong hydrochloric acid was poured into a 100 mL beaker containing about 1 g of zeolite. The solution was accurately transferred to a 100 mL volumetric flask, poured into a beaker and allowed to settle after being carefully directed until the green color disappeared. A volumetric flask was filled with 20 mL of the clear solution, 1 mL of salicylic acid, and 7 mL of buffer solution (or a solution containing 2 mL of 7.6 mM of 1,10-phenanthroline monohydrate and 5 mL of 1.0 M sodium acetate). The mixture was then titrated till the end point against a standard EDTA solution (0.01 M). The titration was repeated until two successive readings were consistent. The number of moles and mass in grams were computed from the titration, and the percentage was calculated. As a point of comparison, the same digested solution was also analyzed for iron using a UV visible spectrophotometer, with the results expressed as a percentage of ferric oxide. Aluminum oxide percentage was computed as the combined oxides percentage minus ferric oxide percentage. The ratio of silicon to aluminum was further computed from the resulting percentages of the respective oxides.

Porosity of the natural zeolite was determined by water displacement method. About 10 g of crushed dry zeolite was measured into falcon tubes in triplicate. About 10 mL of deionized water was added to each tube. The tube was gently shaken and left to stand for 24 h. The final volume of the solution in the tube was recorded. The difference between weight of the initial total solution and the final solution was recorded and taken as total pore volume. Porosity was given by the ratio of pore volume to total volume in percentage. Here, note that 1 g of water is equal to the weight of

1 mL of water. In other words, the density of water is equal to the weight of water.

To determine the pH of the natural zeolite, a known volume of sample after the determination of porosity was used. A pH meter (Consort C6010) was first calibrated using pH 4 and 7 standards and the probe was dipped in a well agitated water bearing sample of natural zeolite. The next step was to wait for the pH probe measurement to stabilize before recording the pH reading. The pH of the deionized water used was also determined for comparison.

To determine the thermal stability of the natural zeolite, about 2 g of the zeolite powder was weighed into two different ceramic crucibles and thereafter subjected to different temperatures over the range 200–800 °C. While weighing after every 1 h of residence time, the loss in weight was determined.

2.2.3 Modification of natural zeolite

Crushed natural zeolite was modified following a surfactant modification method as described in a relevant previous study [16]. Modified zeolite was produced by treating the natural zeolite with 5 g L⁻¹ of hexadecyltrimethylammonium bromide solution in the proportions of 1:100 (zeolite to surfactant solution) in a 2000 mL glass-measuring cylinder. Next, the slurry was washed in distilled deionized water, transferred into ceramic crucibles, and heated at 105 ± 3 °C in an oven (Thermostat Oven DHG-9023A) for 24 h to dryness.

2.2.4 Use of zeolite to remove As(III)

To make a synthetic arsenic nitrate solution, 0.1 g of As(III) oxide (As_2O_3) was digested with 30 mL of 0.1 M of sodium hydroxide solution and dissolved in distilled water up to the 2000 mL volumetric mark. Different contact times of 5 to 30 min were considered. To 45 mL of the synthetic solution, crushed modified zeolite powder of 1 g was added. The resultant solution was left to react for specified 5 min. The solution was filtered and a spectrophotometer was used to determine the adsorbed amount. The adsorption was computed as the ratio of the difference between the initial and final arsenite concentration as a percentage of the initial concentration. The experiment was repeated three times. The entire procedure was repeated with 2 to 10 g of zeolite and contact times in the range 5–30 min.

2.2.5 Use of zeolite to remove lead

To prepare and standardize the lead test water solution, samples were prepared by weighing 100 mg of Pb(II) nitrate and dissolved in 1000 mL of deionized water. Sample solutions were prepared using a micropipette and immediately measured using UV spectroscopy. Five

calibration standards of lead ranging from 10 to 50 mg L⁻¹ were prepared for preliminary calibration of the spectrophotometer. A quartz cuvette with path length of 10 mm was used as the sample container. For every sample, the absorbance of the sample was measured at wavelengths of 205, 211 and 215 nm denoted as D_{205} , D_{211} , and D_{215} , respectively. The cuvettes were washed thoroughly with distilled water to prevent any left over from previous sample. Both the spectrophotometer and deuterium lamp were warmed up for at least 30 min before starting the measurement. The final concentration of lead in each test solution was calculated following the method from a previous study [17] using

$$C_{Pb} = -9.47D_{205} + 18.3D_{211} + 26.4D_{215} + 0.0092 \tag{1}$$

To 45 mL of the solution, 1 g of crushed natural zeolite powder was added. The resultant solution was left to react for specified 10 min. After filtering the solution, the spectrophotometer was used to determine the adsorbed amount. The removal efficiency in percentage was calculated in terms of the difference between initial and final Pb(II) concentration divided by the initial concentration times 100. The experiment was repeated three times and average adsorbed amount considered. The entire procedure was repeated with 3, 5, and 7 g of zeolite and contact times of 40, 60, and 80 min.

2.2.6 Use of zeolite to remove fluorides

The first step involved dissolving 8.4 g of sodium fluoride in 200 mL of distilled deionized water into a 2000 mL volumetric flask and topped to mark with distilled deionized water to make 100 ppm fluoride stock solution. To 45 mL of the solution, 1 g of crushed modified zeolite powder was added. The resulting solution was left to react for specified time (5–30 min). The mixture was

filtered, and the concentration of fluoride in the filtrate was determined by UV/Vis spectrophotometer (Genesys 10S) at a fixed wavelengths of 484 and 664 nm. The overall removal efficiency of the study was calculated in terms of the difference between the initial and final fluoride concentration divided by the initial concentration times 100. The experiment was repeated with 2 to 10 g of modified zeolite for contact times ranging from 5 to 30 min.

2.2.7 Statistical significance of removal of lead, As(III), and fluoride

Two-factor ANalysis Of VAriance (ANOVA) was conducted using heavy metal removal efficiencies. ANOVA without replication was applied because for each contact time, there were three values that were averaged for a particular zeolite dosage. Thus, for each contact time, only one set of lead removal efficiencies (mean values) was summarized for the various zeolite dosages. Similarly, for a given zeolite dosage, there was one set of the mean values for the lead removal efficiencies under each selected contact time. The null hypotheses were that the means of removal efficiencies group by contact time and adsorbent dosage were not different.

3 Results and discussion

3.1 Observed turbidity and synthetic turbid water

Figure 2 shows turbidity in each of the selected months. The lowest, mean and highest turbidity values based on water sampled from the dam are 5, 23 and 103 NTU, respectively (Fig. 2). The mean ± standard deviation of the turbidity values in February, March, April and May were 9.6 ± 6.4, 19.1 ± 6.4, 44.2 ± 29.7, and 15.3 ± 4.0 NTU, respectively. The mean ± standard deviation of turbidity from February to April 2022 was 8 ± 22 NTU. The highest turbidity (103 NTU) was obtained in April. The

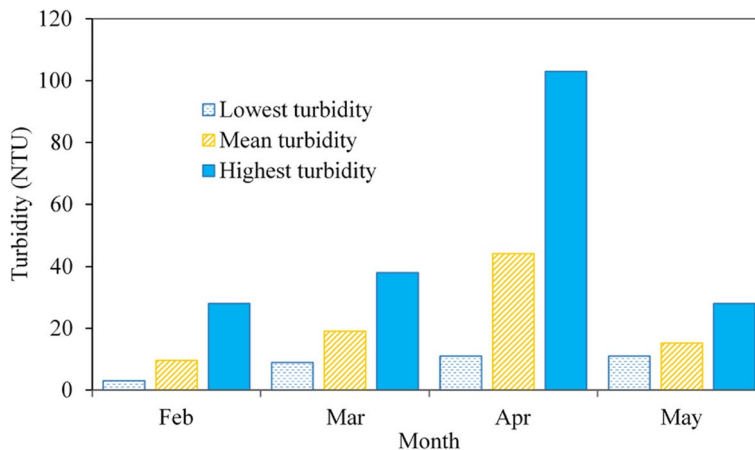


Fig. 2 Turbidity of raw water in a dam at Kamuli water treatment plant in Uganda

lowest turbidity value was 5 NTU and obtained in February. Generally, high turbidity in April was due to the high rainfall intensities. Low values were in February as a month within a dry season. Variation of monthly pollution of surface water sources can be linked to rainfall seasonality. Values of coefficient of variation of the observed turbidity were 0.67, 0.38, 0.67, and 0.26 for February, March, April, and May, respectively.

The lower and upper limits of the values considered for preparing synthetic turbid water were 5 and 120 NTU, respectively. Turbidity of 120NTU was obtained as the standard deviation plus the difference between the highest and lowest turbidity values for water sampled in the dam from February to April 2022 (or $22 + (103 - 5) = 120$). Turbidity in some water sources such as dug well in rural areas can go beyond 120 NTU (see e.g. [18]). Turbidity in various fish landing sites across Uganda monitored from February 2015 to January 2016 considering both dry and wet seasons ranged, on average, from 6.4 ± 2.6 NTU (Majanji, Lake Victoria) to 175 ± 34 NTU (Kahendero, Lake George) [19].

Figure S1 in Supplemental Materials shows scatter plot of clay soil masses versus resultant turbidity values. The equation of the regression line characterizing the variation of observed turbidity (T_0) with clay soil mass (M) was given by

$$T_0 = 81.979M - 1.154 \tag{2}$$

and the units of T_0 and M are NTU and mg L^{-1} , respectively. The coefficient of determination (R^2) close to 1 indicated good performance of the linear model. Eventually, Eq. (1) was used to determine the clay masses for selected turbidity values to be used in the experiment for SDO. Finally, Eq. (2) was ensured to be valid over the range of observed turbidity values obtained in section 3.1.

3.2 Optimization of sand depth

Figure 3 shows results of turbidity removal from synthetic turbid water. Generally, the higher the turbidity, the greater the amount removed (Fig. 3a). The dashed horizontal line indicating turbidity of 5 NTU (or $W\text{-Rlim}$) falls above the entire curve for the turbidity values for the sand depths of 700 and 950 mm (Fig. 3a). This means that the efficiency of turbidity removal increases with the increasing sand depth. Reducing sand depth leads to decrease in the sand grains' surface area and in this way, the overall capacity to adsorb impurities decreases. The main challenge is that as the sand depth is increased, the time taken to get one liter of filtered water increases.

The $W\text{-Rlim}$ cuts the curves for turbidity values based on 200 and 450 mm sand depths. However, considering T_1 values of 60 to 120 NTU, the horizontal line falls between curves for turbidity values based on 450 and 700

mm sand depths. This means that an optimal value exists between 450 and 700 mm. When the s_{opt} is used, T_1 over the range 60–120 NTU is expected to be reduced to final turbidity values less than 5 NTU.

For a given sand depth, efficiency of turbidity removal increases with increasing T_1 (Fig. 3b). Furthermore, for a high T_1 , the efficiency with which the suspended particles can be removed is large. Generally, a large sand depth offers increased sand grains' surface area to trap suspended particles in water. In a highly turbid water, the number of suspended particles is large. The particles, depending on their nature, can stick to each other and this leads to growth in the overall size (flocs). For a given sand depth, low turbidity offers the few suspended particles minimal chances of sticking together and this leads to reduced flocculation.

Figure 4 shows different models fitted to the turbidity values after filtration. The curves for exponential and logarithmic models are comparable. Nevertheless, the models captured the variation of turbidity with sand depths to varying extents. This shows the uncertainty due to the choice of a particular model on the modelling results. The parameters of the various models fitted to the turbidity values are summarized in Table 1.

Statistical model performance (Table 2) shows that the smallest MSE and highest R^2 were obtained using the exponential function regardless of the T_1 values. Thus, the variation of final turbidity with sand depth was best captured by the exponential function. The second-best model was that based on logarithmic function. The MSE values for the linear model were smaller than those from the power model. In other words, the linear model performed better than power model in this study.

The s_{opt} values based on exponential model considering the various T_1 values of 60, 80, 100, and 120 NTU were 453, 522, 561, and 580 mm, respectively. The variation in s_{opt} in mm obtained using the exponential model with T_1 values over the range 60–120 NTU can be described using

$$s_{\text{opt}} = 184 \times \ln(T_1) - 295 \tag{3}$$

The value of R^2 for the relationships between s_{opt} and T_1 based Eq. (3) was 0.996. For Eq. (3) to be applied, the dimensions of the experimental prototype used in this study and those of the practical SSF being considered should be geometrically similar (or have the same linear scale ratio). The limitations of the developed model are that: (i) its extrapolation for turbidity > 120 NTU may yield unreliable results, and (ii) it can be unreliable if the dimensions of the experimental prototype used in this study and the SSF being considered are geometrically dissimilar. Furthermore, the model does not take into consideration other factors that could influence turbidity

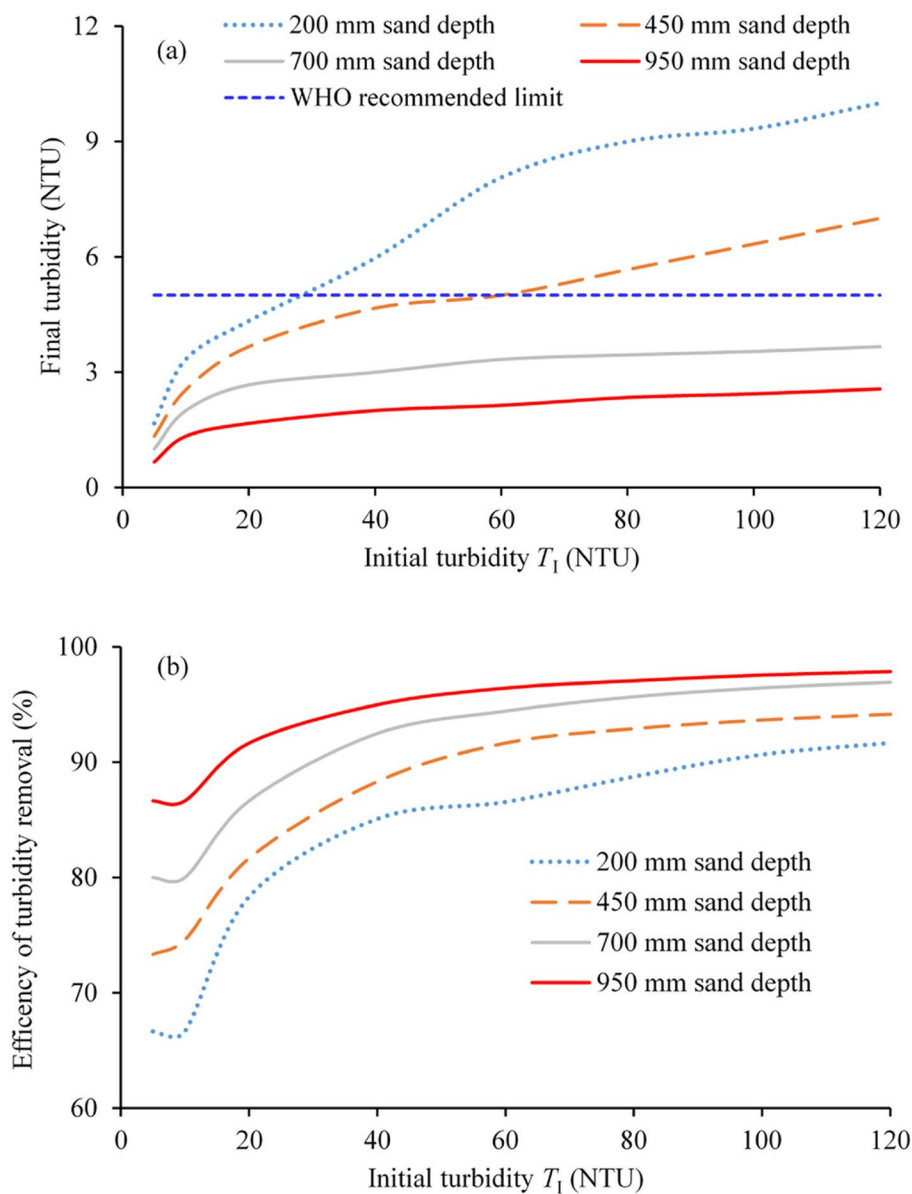


Fig. 3 Turbidity (a) level (NTU) and (b) removal efficiency (%)

removal such as grain size of the particles, nature of the suspended particles causing turbidity, and flow rates. We recommend that these factors should be taken into consideration during future research studies to optimize depths of SSF for turbidity removal.

3.3 Presence of heavy metals and fluorides in raw water from the dam

Table 3 shows presence of total arsenic (As) and heavy metals in the raw water from the dam. Note that As is the sum of arsenite (As(III)) and arsenate (As(V)). Chromium, copper and iron had their concentrations below

the corresponding WHO limits (or W-Rlims). However, the concentrations of arsenic, lead, zinc, manganese, and cadmium were above the W-Rlims. According to WHO, the maximum allowable value of arsenic or lead is 0.01 mg L^{-1} . Metalloids and heavy metals are known to cause numerous diseases which affect various organs in a human body [5]. Even little doses of lead and arsenic can be extremely harmful to human health. These results show the need for removal of heavy metals when treating rainfall-runoff impounded in a dam.

Though not tested in the sampled water, fluoride was found by many researchers [9, 20–23] to occur in water

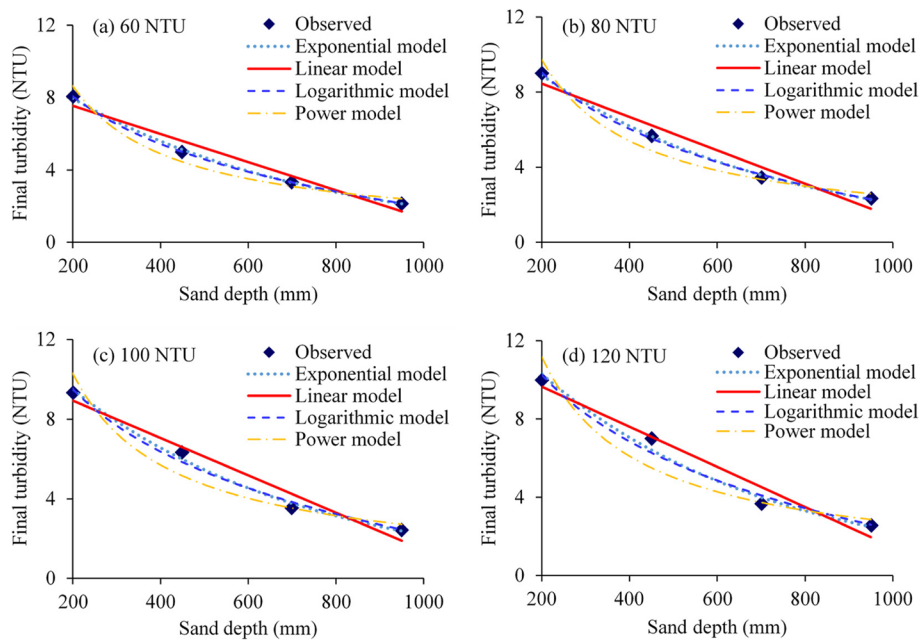


Fig. 4 Final turbidity when T_1 was (a) 60, (b) 80, (c) 100, and (d) 120 NTU

Table 1 Model parameters

Model	T_1	Parameter			
		60 NTU	80 NTU	100 NTU	120 NTU
Exponential $T_F = a \times \exp(b \times s)$	a	113×10^{-1}	128×10^{-1}	137×10^{-1}	150×10^{-1}
	b	-1.7×10^{-3}	-1.8×10^{-3}	-1.8×10^{-3}	-1.9×10^{-3}
Logarithmic $T_F = c \times \ln(s) + d$	c	-3.8	-4.3	-4.5	-4.9
	d	28.2	32	33.5	36.3
Linear $T_F = e \times s + f$	e	-0.01	-0.01	-0.01	-0.01
	f	9.1	10.2	10.8	11.7
Power $T_F = g \times s^h$	g	672	876	962	1156
	h	-0.82	-0.85	-0.86	-0.87

T_F denotes final turbidity (NTU) and s is the sand depth (mm)

from various parts of Uganda as a country in which the raw water was sampled. In many cases, the concentrations of fluoride were found to be greater than the W-Rlim of 1.5 mg L^{-1} . For instance, varying concentrations of fluoride were found across Uganda especially at Sukulu Hills, Tororo District ($0.2\text{--}3 \text{ mg L}^{-1}$) [9], Bunyangabu District ($0.5\text{--}3 \text{ mg L}^{-1}$) [23], Eastern Uganda ($> 1.5 \text{ mg L}^{-1}$) [20], Chuho kisoro ($2.45 \pm 0.01 \text{ mg L}^{-1}$ on average) [22], and Kabale District ($0.3\text{--}0.6 \text{ mg L}^{-1}$) [21].

3.4 Properties of zeolite

The silicon dioxide (SiO_2) and aluminum oxide (Al_2O_3) percentage concentrations in the zeolite sample were 43.5 and 36.5%, respectively. The combined percentage of Al and Si in the zeolite was 80%. This showed that the mineral used was zeolite (a hydrated aluminosilicate

Table 2 Model performance statistics

Model	60 NTU		80 NTU		100 NTU		120 NTU	
	MSE	R^2	MSE	R^2	MSE	R^2	MSE	R^2
Exponential	0.01	0.99	0.001	0.99	0.23	0.96	0.2	0.96
Logarithmic	0.01	0.99	0.01	0.98	0.31	0.95	0.30	0.96
Linear	0.06	0.99	0.09	0.98	0.25	0.96	0.61	0.94
Power	0.14	0.98	0.19	0.97	0.31	0.96	0.94	0.93

Table 3 Concentration of selected heavy metals in raw water from a dam

Metal (loid)	Concentration in raw water (mg L ⁻¹)	W-Rlim or WHO standard (mg L ⁻¹)
Arsenic (As)	0.26	0.01
Lead (Pb)	0.30	0.01
Zinc (Zn)	4.82	3.0
Manganese (Mn)	3.25	0.1
Cadnium (Cd)	0.08	0.003
Chromium (Cr)	0.02	0.05
Cobalt (Co)	0.05	Not provided
Copper (Cu)	0.26	2.0
Iron (Fe)	0.21	0.3

mineral) with silicon and aluminum cations surrounded by four oxygen atoms.

The median pH of the zeolite sample was 8.38, which is greater than 7 and thus, alkaline. Porosity (or a measure of the void space) of the zeolite was 45%. The weight loss of zeolite with temperature was found to be small hence zeolite used in this study was stable from room

temperature to 800 °C. The zeolite had a stable crystal structure. Thus, the zeolite was suitable for applications requiring even elevated temperature.

3.5 Use of zeolite to remove As(III) from synthetic water

Figure 5 shows efficiency of removal of As(III) from synthetic water. For a particular zeolite mass, As(III) removal generally increases with increasing contact time (Fig. 5a). Furthermore, the removal generally increases with the increasing zeolite mass (Fig. 5b). For instance, increasing zeolite mass from 1 to 10 g based on the contact time of 10 min led to an increase of removal efficiency from 76 to 91%.

Table S1 shows results of ANOVA conducted on the efficiency of As(III) removal. The computed *F*-stat is greater than *F*-crit. Thus, the null hypotheses were rejected at $\alpha = 0.05$. Thus, the means of As(III) removal efficiencies grouped by either contact time or zeolite dosage were significantly ($p < 0.05$) different.

Adsorption of As(III) by zeolites stems from the exchange between aluminon hydroxyl groups and adsorbate anionic species [24–27]. In this study, the mean of removal efficiencies considering zeolite mass in the range 1–10 g and contact times varying from 5 to 30

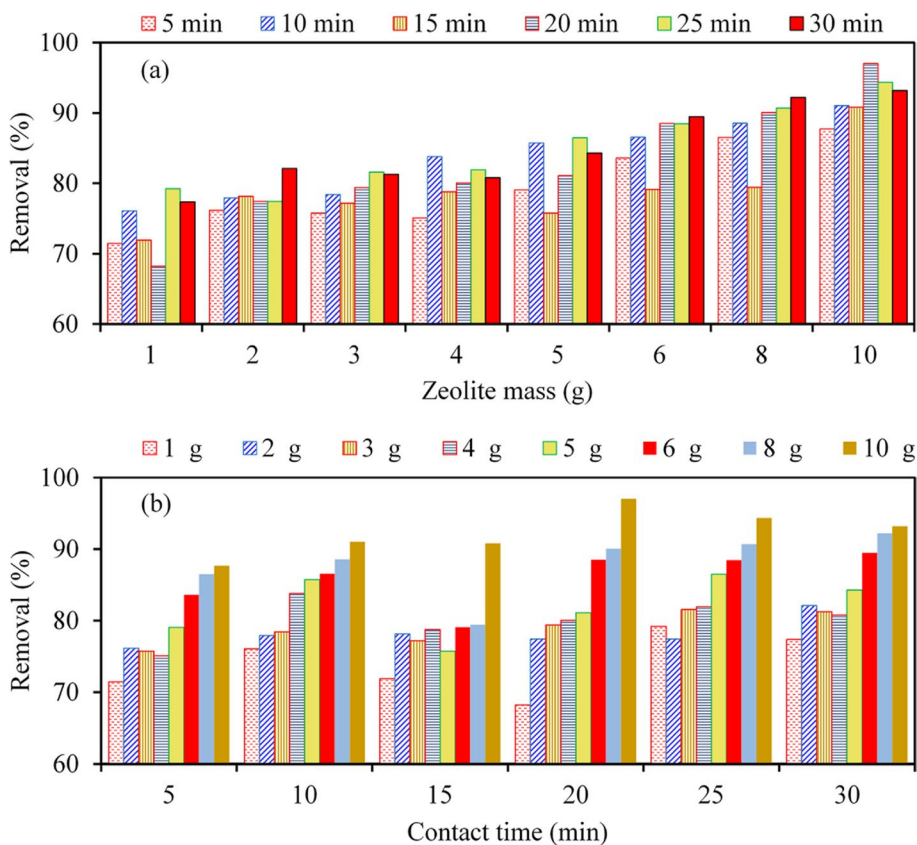


Fig. 5 Removal (%) of arsenic in terms of (a) zeolite mass dissolved in 45 mL of distilled water, and (b) contact time

min was 82%. The minimum and maximum removal efficiencies were 68 and 97%, respectively. In relation with the case of arsenate [28], the adsorbed amount of arsenite from drinking water using zeolite depends on the initial arsenite concentrations. The lower the initial arsenite concentration, the greater the adsorption. In other words, removal efficiency decreases as the concentration of arsenite increases [25]. Apart from initial concentration, efficiency of arsenite removal from water can be affected by other factors such as adsorption agent used, and method of treatment of adsorption agent, dosage of the adsorption agent, pH, and temperature. This study did not focus on all these factors except contact time and dosage of the adsorbent. Thus, this study showed that the amount of arsenite adsorbed in drinking water significantly ($p < 0.05$) depends on both the mass of zeolite and contact time (Table S1).

3.6 Use of zeolite to remove lead from synthetic turbid water

Figure 6 shows efficiency of Pb(II) removal using zeolite from synthetic water. Using 1 g of zeolite dissolved in 45 mL of distilled water, Pb(II) removal efficacy of 75% was

achieved considering 20-min contact time. The efficiency increased with increasing contact time up to 60 min. Using 5 g of zeolite, the maximum Pb(II) removal efficiencies of 86 and 98% were obtained for contact times of 20 and 40 min, respectively (Fig. 6a). The differences in lead removal efficiencies based on contact times over the range 40–100 min were smaller than those considering 20–40 min (Fig. 6b). The highest efficiency for 20-min contact time was obtained using 5 g of zeolite.

Table S2 shows statistical results of ANOVA conducted on the efficiency of Pb(II) removal. It can be seen that F -stat is greater than F -crit. Thus, the null hypotheses were rejected at $\alpha = 0.05$ meaning that the means of lead removal efficiencies grouped by either contact time or zeolite dosage were significantly ($p < 0.05$) different.

Several studies investigated affinity of zeolite for lead [29, 30]. Lead removal efficiency using Iranian natural zeolite was close to 100% within 40 min [29]. Adsorption of lead onto zeolite from ‘Beli Plast’ mine (Bulgaria) was up to 99% [30]. Apart from contact time and mass of the zeolite, there are other factors shown to affect the efficiency of zeolite in removal of lead including zeolite particle size [31], initial concentration [30], method of

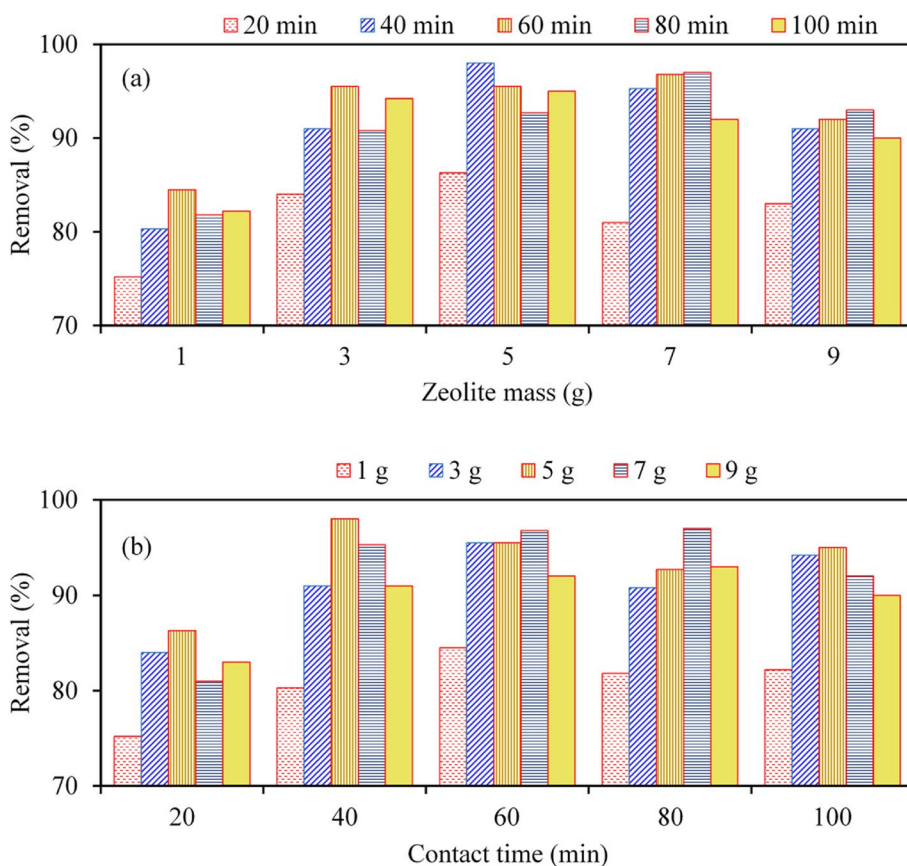


Fig. 6 Removal (%) of lead in terms of (a) zeolite mass dissolved in 45 mL of distilled water, and (b) contact time

zeolite modification [32], and variation in the number of competing ions [29]. Despite the various factors, zeolites from various origins or sources across the world are different from one another in some particular aspects. Thus, adsorption efficiency of a particular zeolite could be influenced by the choice of the source from which it is obtained.

3.7 Use of zeolite to remove fluorides from synthetic water

Figure 7 shows efficiency of removal of fluorides from synthetic water. For a given zeolite mass, removal efficiency increased with increasing contact time. Removal efficiencies increased over ranges 28–80 and 41–84% for contact times of 5 and 25 min, respectively (Fig. 7a). Differences in removal efficiencies for 1 and 10 g of zeolite were 52 and 43% for contact times of 5 and 30 min, respectively (Fig. 7a). For a particular contact time, removal increased with increasing zeolite mass (Fig. 7b). For instance, fluoride removal efficiencies using 1, 3, 5, and 10 g of zeolite dissolved in 45 mL based on 5-min contact time were 28, 38, 53, and 80%, respectively.

Table S3 shows results of ANOVA for removal of fluoride from water. The computed *F*-stat is again greater than *F*-crit. Therefore, the null hypotheses

were rejected at $\alpha = 0.05$. Thus, the means of fluoride removal efficiencies grouped by either contact time or zeolite dosage were significantly ($p < 0.05$) different.

The use of zeolite to remove fluoride in water was investigated in several studies. For instance, 2 g of Mn-Ti modified zeolite yielded about 77% fluoride removal from water [16]. Stilbite zeolite modified with FeCl₃ solution yielded maximum fluoride adsorption capacity is 2.31 mg g⁻¹ [33]. Zeolite conditioned with iron was able to remove up to 98% of fluoride in water [34]. Iron and zirconium doped zeolite removed over 80% of fluoride when the initial concentration was less than 20 mg L⁻¹ [35]. In treating water with fluoride initial concentration of 1.63 mg L⁻¹, aluminum modified zeolite was able to reduce the fluoride ion to less than 1 mg L⁻¹ [36]. From the above results, it can be realized that the efficiency of zeolite in removal of fluoride depends on the method of zeolite modification. Furthermore, removal of fluoride using unmodified zeolite is far less than that when based on modified zeolite [14]. Results of this study (Fig. 7) showed the fluoride removal also depends on contact time and concentration of zeolite (or adsorbent dose). Other factors (not considered in this study for brevity) that also affect

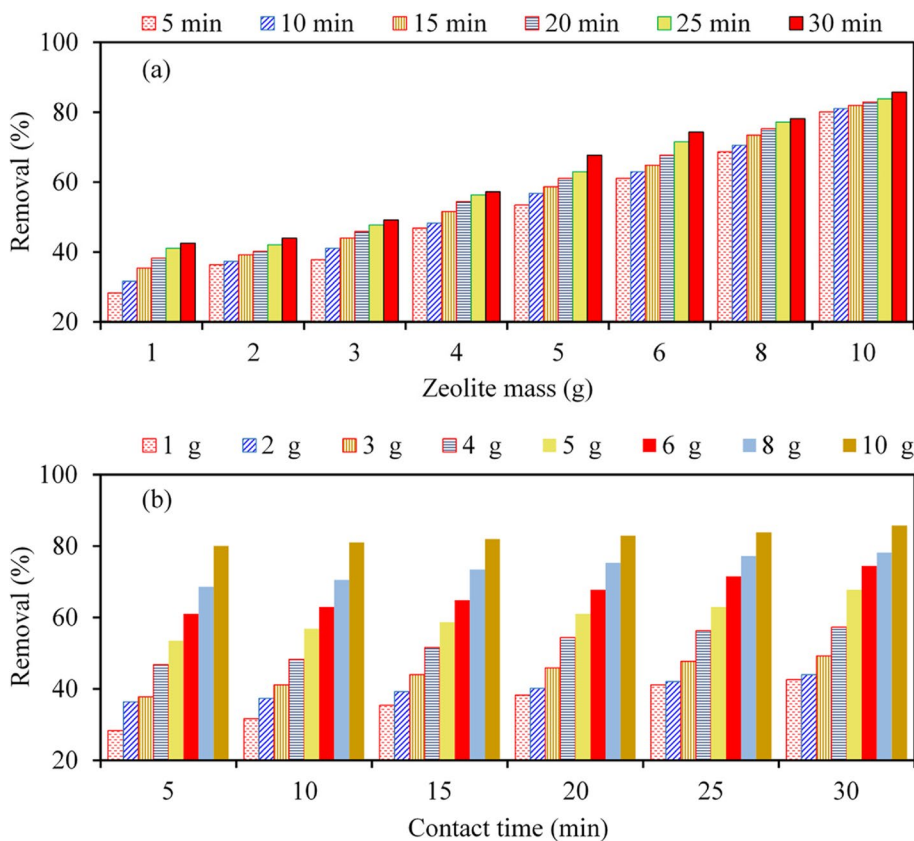


Fig. 7 Removal (%) of fluoride in terms of (a) zeolite mass dissolved in 45 mL of distilled water, and (b) contact time

removal of fluoride using zeolite include pH, temperature, and initial concentration [37].

3.8 Practical application of zeolite in the water treatment

The incorporation of zeolite into water treatment system could be done in a number of ways. Firstly, the crushed zeolite could be incorporated as a layer sandwiched between the sand and gravel layers (see for instance [25]). In such a case it becomes difficult to take into account the effect of contact time on the efficiency of removing targeted pollutants such as heavy metals. Figure 8 shows the second option in which the crushed zeolite is used to treat filtrate from the SSF. This study recommended the second option. Water from the dam (A) is directed to an aerator (B), and passed to the SSF (C). The effluent from the SSF is directed into tank D for dosing of zeolite and agitation of the resultant solution. When the agitation time is achieved, the resultant solution is passed to tank E with two compartments E₁ and E₂. Compartment E₁ is for achieving the targeted contact time. Compartment E₂ is for sedimentation and subsequent filtration of the zeolite residue. The filtrate is directed to the disinfection tank (F) from which the treated water is pumped into the reservoir (H) for supply to the distribution network (I) by gravity. For an existing water treatment and supply system, the additional cost for treatment of heavy metals would be that for incorporating the tank(s) for zeolite dosing and its subsequent sedimentation or filtration.

Analyses of costs for treating wastewater using various classes of adsorbents were reviewed in a recent study [11]. The costs of treating wastewater using any adsorbents (such as natural and modified zeolite) at < 1 USD mol⁻¹ and > 200 USD mol⁻¹ were regarded to be cheap and very expensive, respectively [11]. These costs were developed for the period 2016–2021 and they will need

to be revised to reflect eventualities such as the effect of COVID pandemic and inflation.

4 Conclusions

Experiments for sand bed depth optimization were conducted using SSF metallic prototypes each having 300 × 300 × 1700 mm dimension with 200 mm underdrain gravel layer. Variation of final turbidity with sand bed depth was found to be best described by an exponential function. The optimal sand bed depth on top of underdrain gravel layer of 200 mm when water to be treated had turbidity of up to 120 NTU was about 585 mm. The turbidity removal efficiency was found to depend on the initial turbidity. In other words, the turbidity removal efficiency of a highly turbid water is high. However, removing high turbidity requires a large sand depth. The optimal sand bed depths when turbid water had turbidity values of 60, 80, 100, and 120 NTU were 453, 522, 561, and 580 mm, respectively. For brevity, other factors which affect turbidity removal such as the size of the filter particles, and flow rates, were not considered but should be taken into account in future research studies.

Removal of lead, As(III), and fluorides indicated promising potential of the natural zeolites from Uganda for treating water polluted with heavy metals. Lead removal efficiencies using natural zeolite under 20 and 40 min were 75 and 98%, respectively. Removal of As(III) using modified zeolite was 91% within contact time of 10 min. Removal of fluoride using modified zeolite was 80% within 5 min. For a selected zeolite mass, fluoride removal was noted to generally increase with increasing contact time. The removal efficiencies of lead, As(III), and fluorides were also shown to increase with the increasing zeolite mass. Worth noting is that this study separately conducted investigations for the removal of lead, As(III), and fluorides on zeolite. If Pb(II), As(III), and fluorides

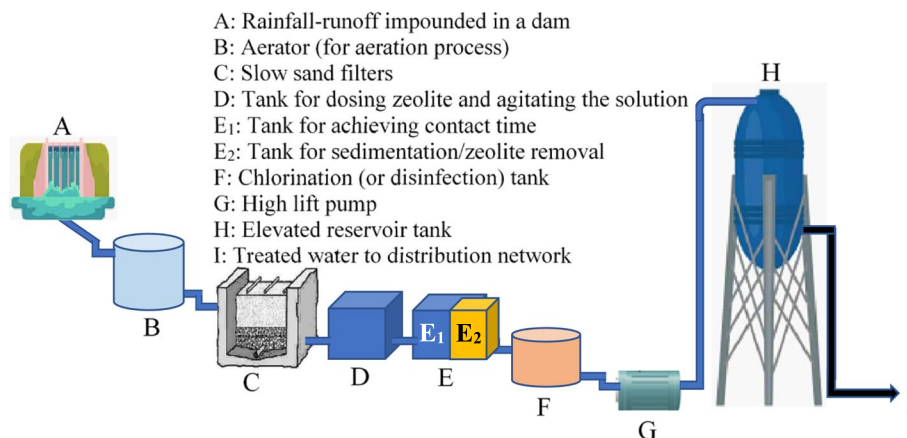


Fig. 8 Incorporating zeolite in water treatment system

were mixed into one solution, competitive removal would have taken place. In a previous study using Iranian natural zeolite, removal of lead reached 100% under 40 min and it took about a day for the adsorption kinetics for other ions including cadmium, copper, and nickel ions to reach equilibrium state [29]. However, when the metals were separately considered, adsorption of copper, nickel, cadmium and lead ions reduced to 90, 53, 30, and 22%, respectively [29]. Thus, determination of adsorption rates of the Ugandan zeolites for multi-component solutions is recommended for comprehensive analysis under future research.

Using optimized sand depth, a saving of up to 35% of the total cost for acquiring sand required by a conventional SSF was achieved with at least 95% efficiency in removing turbidity as high as 120 NTU. Normally, the filter of SSF tends to clog over time due to increasing population of microorganisms and this leads to reduction in the flow rates thereby requiring maintenance. To remove the material clogging the filter media, a thin layer of the biofilm is scraped. The scraped filter layer can be cleaned and recycled. The frequencies with which scraping should be undertaken in the two cases when the sand bed depth of the SSF is optimized and unoptimized can be different and this was not investigated in this study. Thus, both the short- and long-term costs of using optimized and unoptimized sand depth should be investigated in future research.

We also recommend separate research to investigate the overall cost of applying zeolite for water treatment while taking into account relevant factors such as the adsorbent's processing cost, adsorbent's life time (or the rate at which a particular adsorbent degenerates), adsorption capacity, inflation, unit cost of energy, initial (or installation) and operational cost. To optimize removal of heavy metals from pollutants, we recommend an investigation of the use of nano-zeolite compared with activated carbon. The cost of nano-zeolite to remove nitrophenol from wastewater was found to be 0.03 USD g⁻¹ and this is far cheaper than using activated carbon with the further advantage that reusage of nano-zeolite could go up to five times [38].

Supplementary Information

The online version contains supplementary material available at <https://doi.org/10.1186/s42834-024-00209-x>.

Supplementary Material 1.

Acknowledgments

The authors acknowledge that results on SDO and adsorption experiment for removal of Pb(II) were partially based on the dissertation of Emmanuel Okello [39]. Results of adsorption experiments for Pb(II), fluoride and As(III) were partially based on dissertations of Rebecca Atukwase, Pamela Nduhukiire, and Michael Ecodu from the Department of Civil and Environmental Engineering,

Kyambogo University. The experiments for investigating the potential of zeolite for removal of Pb(II), As(III) and fluoride were conducted from the Chemistry laboratory of Kyambogo University. The authors are grateful to Mr. Olado Simon Peter of the Chemistry laboratory of Kyambogo University for the technical support he provided during adsorption experiments. Concentrations of As, Pb(II), manganese, cadmium, chromium, cobalt, copper and iron of raw water sampled from the dam in Kamuli were tested in the laboratory of the Department of Geology and Petroleum Studies under the College of Natural Sciences of Makerere University.

Authors' contributions

Onyutha C: Conceptualization, Formal analysis, Investigation, Resources, Data Curation, Writing, Supervision - Original Draft, Review & Editing, Visualization; Okello E: Conceptualization, Formal analysis, Investigation, Resources, Data Curation, Review & Editing, Visualization; Atukwase R: Investigation, Data Curation, Review & Editing; Nduhukiire P: Investigation, Data Curation, Review & Editing; Ecodu M: Investigation, Data Curation, Review & Editing; Kwiringira J N: Reviewed the manuscript and did final editing before submission.

Funding

This research received no external funding.

Availability of data and materials

Data used in this study can be obtain on request from the first or corresponding author of this paper.

Declarations

Competing interests

The authors declare that there are no conflicts of interest of a financial or personal nature.

Author details

¹Department of Civil and Environmental Engineering, Kyambogo University, P.O. Box 1, Kyambogo, Uganda. ²Department of Sociology and Social Administration, Kyambogo University, P.O. Box 1, Kyambogo, Uganda.

Received: 9 July 2023 Accepted: 20 February 2024

Published online: 08 March 2024

References

1. UN. The 17 goals. New York: United Nations; 2015. <https://sdgs.un.org/goals>. Accessed 6 Feb 2024.
2. Freitas BLS, Terin UC, Fava NMN, Maciel PMF, Garcia LAT, Medeiros RC, et al. A critical overview of household slow sand filters for water treatment. *Water Res.* 2022;208:117870.
3. Muhammad N, Parr J, Smith MD, Wheatley AD. Removal of heavy metals from storm and surface water by slow sand filtration: the importance of speciation. *Urban Water J.* 2005;2:33–7.
4. Logsdon GS, Kohne R, Abel S, LaBonde S. Slow sand filtration for small water systems. *J Environ Eng Sci.* 2002;1:339–48.
5. Singh A, Sharma RK, Agrawal M, Marshall F. Risk assessment of heavy metal toxicity through contaminated vegetables from waste water irrigated area of Varanasi, India. *Trop Ecol.* 2010;51:375–87.
6. Mohapatra M, Anand S, Mishra BK, Giles DE, Singh P. Review of fluoride removal from drinking water. *J Environ Manage.* 2009;91:67–77.
7. Jain CK, Singh RD. Technological options for the removal of arsenic with special reference to South East Asia. *J Environ Manage.* 2012;107:1–18.
8. Marshall G, Ferreccio C, Yuan Y, Bates MN, Steinmaus C, Selvin S, et al. Fifty-year study of lung and bladder cancer mortality in Chile related to arsenic in drinking water. *J Natl Cancer Inst.* 2007;99:920–8.
9. Egor M, Birungi G. Fluoride contamination and its optimum upper limit in groundwater from Sukulu Hills, Tororo District, Uganda. *Sci Afr.* 2020;7:e00241.
10. Wang S, Peng Y. Natural zeolites as effective adsorbents in water and wastewater treatment. *Chem Eng J.* 2010;156:11–24.

11. Ighalo JO, Omoarukhe FO, Ojukwu VE, Iwuozor KO, Igwegbe CA. Cost of adsorbent preparation and usage in wastewater treatment: A review. *Clean Chem Eng.* 2022;3:100042.
12. Rhodes CJ. Properties and applications of zeolites. *Sci Prog.* 2010;93:223–84.
13. Mandoreba C, Gwenzi W, Chaukura N. Defluoridation of drinking water using a ceramic filter decorated with iron oxide-biochar composites. *Int J Appl Ceram Tec.* 2021;18:1321–9.
14. Donkor EA, Buamah R, Awuah BK. Defluorination of drinking water using surfactant modified zeolites. *J Sci Technol.* 2016;36:15–21.
15. Camacho LM, Parra RR, Deng S. Arsenic removal from groundwater by MnO₂-modified natural clinoptilolite zeolite: Effects of pH and initial feed concentration. *J Hazard Mater.* 2011;189:286–93.
16. Yang B, Sun G, Quan B, Tang J, Zhang C, Jia C, et al. An experimental study of fluoride removal from wastewater by Mn-Ti modified zeolite. *Water.* 2021;13:3343.
17. Tan CH, Moo YC, Mat Jafri MZ, Lim HS. UV spectroscopy determination of aqueous lead and copper ions in water. In: SPIE Photonics Europe 2014. Brussels: Society of Photo-Optical Instrumentation Engineers (SPIE); 2014. <https://doi.org/10.1117/12.2052349>.
18. Apecu RO, Ampaire L, Mulogo EM, Bagenda FN, Traore A, Potgieter N. Quality of water sources in Southwestern Uganda using the compartment bag test (CBT): a cross-sectional descriptive study. *J Water Sanit Hyg De.* 2019;9:683–93.
19. Bwire G, Sack DA, Kagirita A, Obala T, Debes AK, Ram M, et al. The quality of drinking and domestic water from the surface water sources (lakes, rivers, irrigation canals and ponds) and springs in cholera prone communities of Uganda: an analysis of vital physicochemical parameters. *BMC Public Health.* 2020;20:1128.
20. Jovine M, Edikafubeni M, Alfred NNM. Fluoride Levels in Surface and Groundwater in Africa: A Review. *Am J Water Sci Eng.* 2017;3:1–17.
21. Ngabirano H, Byamugisha D, Ntambi E. Temporal and spatial seasonal variations in quality of gravity flow water in Kyanamira Sub-County, Kabale District, Uganda. *J Water Res Prot.* 2017;9:455–69.
22. Nkurunziza G, Omara T, Nakiguli CK, Mukasa P, Byamugisha D, Ntambi E. Physicochemical quality of water from Chuho Springs, Kisoro District, Uganda. *Fr Ukr J Chem.* 2021;09:12–26.
23. Wozzi E, Nasasira B, Kugonza B. Household-level Fluoride reduction from drinking water using crushed fired clay – proof of concept. *Int J Biol Chem Sci.* 2021;15:82–9.
24. Soni R, Shukla DP. Data on Arsenic(III) removal using zeolite-reduced graphene oxide composite. *Data Brief.* 2019;22:871–7.
25. Abdolhnejad A, Jafari N, Ebrahimi A, Mohammadi A, Farrokhzadeh H. Removal of arsenic and coliform bacteria by modified sand filter with slag and zeolite from drinking water. *Health Scope.* 2017;6:e15170.
26. Lizama-Allende K, Henry-Pinilla D, Diaz-Droguett DE. Removal of arsenic and iron from acidic water using zeolite and limestone: Batch and column studies. *Water Air Soil Poll.* 2017;228:275.
27. Pinedo-Torres LA, Bonilla-Petriciolet A, Garcia-Arreola ME, Villagrana-Pacheco Y, Castaneda-Miranda AG, Berber-Mendoza MS. Adsorption of arsenic, lead, cadmium, and chromium ions from aqueous solution using a protonated chabazite: Preparation, characterization, and removal mechanism. *Adsorpt Sci Technol.* 2023;2023:2018121.
28. Bilici Baskan M, Pala A. Removal of arsenic from drinking water using modified natural zeolite. *Desalination.* 2011;281:396–403.
29. Merrikhpour H, Jalali M. Comparative and competitive adsorption of cadmium, copper, nickel, and lead ions by Iranian natural zeolite. *Clean Technol Environ.* 2013;15:303–16.
30. Shaheen SM, Derbalah AS, Moghanm FS. Removal of heavy metals from aqueous solution by zeolite in competitive sorption system. *Int J Environ Sci Dev.* 2012;3:362–7.
31. Wingenfelder U, Nowack B, Furrer G, Schulin R. Adsorption of Pb and Cd by amine-modified zeolite. *Water Res.* 2005;39:3287–97.
32. Yuan M, Xie T, Yan G, Chen Q, Wang L. Effective removal of Pb²⁺ from aqueous solutions by magnetically modified zeolite. *Powder Technol.* 2018;332:234–41.
33. Sun Y, Fang Q, Dong J, Cheng X, Xu J. Removal of fluoride from drinking water by natural stilbite zeolite modified with Fe(III). *Desalination.* 2011;277:121–7.
34. Sampedro-Duran J, Torres-Rodriguez M, Gutierrez-Arzaluz M, Mugica-Alvarez V. Removal of fluoride in water with Mexican natural zeolite. *Proceedings.* 2018;2:1470.
35. Yang B, Jia C, Sun G, Quan B, Zhang C, Huo Q, et al. Enhancing the adsorption function of F⁻ by iron and zirconium doped zeolite: Characterization and parameter optimization. *Environ Eng Res.* 2023;28:220010.
36. Yafeng LI, Wenqing L. Preparation of aluminium modified zeolite and experimental study on its treatment of fluorine-containing water. *IOP C Ser Earth Env.* 2018;199:032023.
37. Panda L, Kar B, Dash S. Preparation of fly ash based zeolite for removal of fluoride from drinking water. *AIP Conf Proc.* 2018;1953:080003.
38. Pham TH, Lee BK, Kim J. Improved adsorption properties of a nano zeolite adsorbent toward toxic nitrophenols. *Process Saf Environ.* 2016;104:314–22.
39. Okello E. Improving Slow Sand Filtration Through Sand Depth Optimization and Lead Removal Using Zeolite: Case of Kamuli Water Treatment Plant [M.Sc. thesis]. Kampala: Kyambogo Univ; 2023.

Publisher's Note

Springer Nature remains neutral with regard to jurisdictional claims in published maps and institutional affiliations.